IEEE Access
Multidisciplinary | Rapid Review | Open Access Journal

Received May 9, 2020, accepted May 26, 2020, date of publication June 5, 2020, date of current version June 16, 2020.

Digital Object Identifier 10.1109/ACCESS.2020.3000273

Spatiotemporal Parameterization of Human Reaching Movements Based on Time Base Generator

MASANOBU KITTAKA[1], AKIRA FURUI[1], (Member, IEEE), HIROTO SAKAI[1], PIETRO MORASSO[2], AND TOSHIO TSUJI[1], (Member, IEEE)

[1]Department of System Cybernetics, Graduate School of Engineering, Hiroshima University, Higashi-Hiroshima 739-8527, Japan
[2]Department of Robotics, Brain, and Cognitive Sciences, Istituto Italiano di Tecnologia, 16163 Genoa, Italy

Corresponding authors: Akira Furui (akirafurui@hiroshima-u.ac.jp) and Toshio Tsuji (tsuji@bsys.hiroshima-u.ac.jp)

ABSTRACT Human reaching movement is characterized by the invariant features of linearity and the symmetrical bell-shaped velocity profile of the hand trajectory. Reaching movement has been widely evaluated in fields such as rehabilitation and interface design; however, no standardized protocols exist for data collection, processing, or analysis. This paper proposes a spatiotemporal parameterization method that evaluates reaching movements with a trajectory generation model based on a time base generator. The proposed method extracts motion information as a set of model parameters, such as motion duration, distance, and asymmetry of the bell-shaped velocity profile from the reaching data, that are estimated by fitting the model to reaching data with a robust parameter estimation method. The reaching trajectory generation model, for which a straight trajectory in a three-dimensional space is assumed, is also derived from the proposed model. Experiments were conducted using simulated data and real-world three-dimensional and one-dimensional human reaching movement datasets. The results show that the model assuming a straight trajectory in the three-dimensional space is reasonable for evaluating reaching movements. In addition, the model parameters were estimated with relatively greater robustness than were those of the conventional model and were highly correlated with physical features extracted from measured datasets. The results also showed that the parameters representing the asymmetry of the bell-shaped velocity profile differed between individuals. Therefore, the characteristics of reaching movements can be parameterized and evaluated with the proposed method.

INDEX TERMS Human reaching movements, time base generator (TBG), trajectory generation model, parameter estimation, motion parameterization.

I. INTRODUCTION

A basic component of everyday human motor repertoire, the reaching movement refers to the movement of the hand from an initial to a target position according to a motivation-based trajectory generated by the brain by taking distance and direction into account. Reaching movements have been evaluated by investigators to help improve motor function in rehabilitation and to inform the design of user interfaces [1]–[5].

Several indices of the reaching movement, such as reaching movement duration, mean velocity, and peak velocity, have been used to evaluate the reaching movement [5]–[7]. However, standardized protocols (e.g., data collection, processing, and analysis) to evaluate upper limb movements remain lacking [5], [6]. Defining the reaching movement time is particularly difficult, as various methods have been used to determine reaching movement time based on the available data, such as extracting at a rate of 5%–20% of the peak velocity, and no one definition of this index exists. In addition, the characteristics of reaching movement depend more heavily on past experiences than on physical traits or age [8]. However, few studies have focused on the analysis and evaluation of individual differences in the shape of the velocity waveform during a reaching movement [8]–[10].

The associate editor coordinating the review of this manuscript and approving it for publication was Kumaradevan Punithakumar.

During a proficient reaching movement, hand trajectory follows a roughly straight path with a symmetrical bell-shaped velocity profile: an invariant feature of reaching movements [11]. To elucidate the mechanisms underlying reaching movement with this common invariant feature, several models of human reaching trajectory generation have been developed, including feedforward models (e.g., the minimum jerk model [12], the minimum torque change model [13], and the minimum endpoint variance model [14]) and feedback models (e.g., the vector integration to endpoint [VITE] model [15]).

As an alternative approach, Morasso *et al.* proposed a time base generator (TBG) to model hand trajectories during reaching movements [16]. The TBG combines feedforward and feedback configurations into a unified framework that can generate a time series with a bell-shaped velocity profile. In consideration of the distortion of the velocity profile due to changes in task environments, Tsuji *et al.* later proposed a TBG that could generate a time series with an asymmetric bell-shaped velocity profile [17]. Tanaka *et al.* further reported that this TBG could be represented by a network of neurons [18].

The TBG is comprised of parameters that express the reaching time and the shape of the velocity profile. Therefore, if the TBG parameters could be estimated from the measurement data of reaching movements, then the bell-shaped profile could also be quantitatively evaluated. To date, however, the TBG has only been applied to trajectory generation for robots [17]–[19], and no attempt has been made to estimate TBG parameters from human data and use them to evaluate reaching movements.

This paper proposes a spatiotemporal parameterization method to evaluate human reaching movements based on the TBG [17]. The proposed method consists of a human reaching trajectory generation model based on the TBG and an estimation method of the model parameters. The parameters of the proposed model can be estimated by minimizing the residual between the velocity profile generated by the model and the measured velocity profile using the nonlinear least-squares method. The accuracy of the model was evaluated using simulated data, and the relationship between the model parameters and the physical features of the reaching movement were analyzed using real-world three- and one-dimensional reaching data. The primary contributions of this paper are as follows:

1) The results of the simulation experiment show that the proposed method can be used for robust parameter estimation for the addition of noise and waveform extraction.
2) The proposed method can quantitatively extract motion information, such as motion duration, distance, and the asymmetry of the bell-shaped velocity profile, as model parameters from reaching data. This is supported by a high correlation between the model parameters and the physical features of the reaching movement, obtained experimentally.
3) Individual differences in the shape of the velocity waveform can be evaluated based on the estimated model parameters.

The remainder of this paper is organized as follows: Section II describes the reaching trajectory generation model based on the TBG and its parameter estimation method; Section III describes the experimental method for model verification and three- and one-dimensional reaching data analysis; Section IV presents the results of these experiments; Section V discusses the results; and Section VI presents the conclusions of this study.

II. SPATIOTEMPORAL PARAMETERIZATION METHOD BASED ON TBG

This section describes the TBG, the reaching trajectory generation model based on the TBG, and the parameter estimation method used to construct the spatiotemporal parameterization method for human reaching movements.

A. TBG

The TBG is represented by the function $\xi(t)$, which is an increasing function satisfying $\xi(0) = 0$ and $\xi(t_f) = 1$. The dynamics of ξ are defined as follows [17]:

$$\dot{\xi} = \gamma \xi^{\beta_1} (1 - \xi)^{\beta_2}, \tag{1}$$

where the parameter γ is a function of the end time t_f, and β_i (i.e., β_1 and β_2) is a positive constant under the condition of $0 < \beta_i < 1$. The function $\xi(t)$ represents the time base trajectory with normalized amplitude and a one-shot time profile. The TBG is similar to a central pattern generator (CPG), but the resulting trajectory is non-periodic. We use $\xi(t)$ to generate the hand position during human reaching movement. Therefore, the feedback control rule in the TBG can generate a trajectory according to which a human hand can reach the target with a bell-shaped velocity profile at the specified time t_f by outputting a command that synchronizes the error between the current position ξ and a normalized target position with TBG. In this instance, the end time t_f can be calculated with the following equation:

$$t_f = \int_0^{t_f} dt = \int_0^1 \frac{d\xi}{\dot{\xi}} = \frac{\Gamma(1-\beta_1)\Gamma(1-\beta_2)}{\gamma\Gamma(2-(\beta_1+\beta_2))}, \tag{2}$$

where $\Gamma(\cdot)$ is the gamma function (i.e., Euler's integral of the second kind). Thus, the convergence time of ξ can be freely adjusted if the parameter γ in (2) is defined as

$$\gamma = \frac{\Gamma(1-\beta_1)\Gamma(1-\beta_2)}{t_f\Gamma(2-(\beta_1+\beta_2))}. \tag{3}$$

B. REACHING TRAJECTORY GENERATION MODEL BASED ON TBG

The TBG can generate symmetric and asymmetric bell-shaped velocity waveforms along the time axis in the same manner that humans actually generate velocity waveforms. However, in many instances, the reaching data is saved

only during the time when the absolute value of the velocity vector exceeds a certain threshold value. Thus, it is unclear whether the start times of data storage and the reaching movement actually coincide. The true starting time and travel distance are consequently unknown, and the conventional TBG cannot express these parameters. We therefore propose a new reaching trajectory generation model based on the TBG that can account for changes in starting time and travel distance.

Assuming that the reaching trajectory generation model for a one-dimensional velocity waveform is obtained during a reaching movement, the velocity signal $\dot{x}$ of hand position x during a reaching movement with a target distance α_x is defined as follows:

$$\dot{x} = \alpha_x \gamma_x \xi_x^{\beta_{1x}} (1 - \xi_x)^{\beta_{2x}}, \tag{4}$$

where the parameter γ_x is a function of the start time t_s and end time t_f, and ξ_x is defined as $\xi_x = x/\alpha_x$. Here, x satisfies $x(t_s) = 0$ and $x(t_s + t_f) = \alpha_x$, and ξ_x satisfies $\xi_x(t_s) = 0$ and $\xi_x(t_s + t_f) = 1$. The end time t_f and the parameter γ_x are defined in the same manner as in (2) and (3) as follows:

$$t_f = \int_{t_s}^{t_s+t_f} dt = \int_0^1 \frac{d\xi_x}{\dot{\xi}_x} = \frac{\Gamma(1-\beta_{1x})\Gamma(1-\beta_{2x})}{\gamma_x \Gamma(2-(\beta_{1x}+\beta_{2x}))}, \tag{5}$$

$$\gamma_x = \frac{\Gamma(1-\beta_{1x})\Gamma(1-\beta_{2x})}{t_f \Gamma(2-(\beta_{1x}+\beta_{2x}))}. \tag{6}$$

Note that t_f is defined as the reaching end time with respect to t_s. The constraints for x in terms of the start and end times, t_s and t_f, are shown in Fig 1.

The acceleration signal $\ddot{\xi}_x$ of the TBG is defined as follows:

$$\ddot{\xi}_x = \gamma^2 \xi_x^{2\beta_{1x}-1} (1-\xi_x)^{2\beta_{2x}-1} (\beta_{1x} - (\beta_{1x}+\beta_{2x})\xi_x). \tag{7}$$

Based on this equation, the velocity signal $\dot{\xi}_x$ has an absolute maximum value at $\xi_x = \beta_{1x}/(\beta_{1x} + \beta_{2x})$. From (7) and $\xi_x = x/\alpha_x$, $\dot{x}$ has an absolute maximum value at $x = \alpha_x \beta_{1x}/(\beta_{1x} + \beta_{2x})$. Indicating the point at which the velocity reaches its maximum with respect to the normalized distance, the expression $\beta_{1x}/(\beta_{1x} + \beta_{2x})$ is defined as the β ratio.

When the β ratio is 0.5, the velocity profile is symmetrical with respect to time. Therefore, the "bell-shapeness" of the velocity profile can be evaluated during reaching movements by using the β ratio.

Fig. 2 shows examples of the time history of x and $\dot{x}$ with $[\beta_1, \beta_2]$ set to [0.75, 0.5], [0.75, 0.75], and [0.5, 0.75] (Fig. 2(a)); t_s set to −0.2, 0, and 0.2 (Fig. 2(b)); and α_x set to 0.2, 0.3, and 0.4 (Fig. 2(c)). The fixed parameters were set to $\alpha_x = 0.3$, $t_s = 0$, and $t_f = 1$ (Fig. 2(a)); $\alpha_x = 0.3$, $t_f = 1$, and $[\beta_1, \beta_2] = [0.7, 0.7]$ (Fig. 2(b)); and $t_s = 0$, $t_f = 1$, and $[\beta_1, \beta_2] = [0.7, 0.7]$ (Fig. 2(c)). As Fig. 2(a) demonstrates, the β ratio value changes to 0.4, 0.5, and 0.6 when β_1 and β_2 change, and the asymmetry of the bell-shaped velocity waveform changes accordingly. This indicates that the asymmetry of the bell-shaped velocity waveform can be quantified with the β ratio. The start time and final distance of a reaching movement are adjusted by

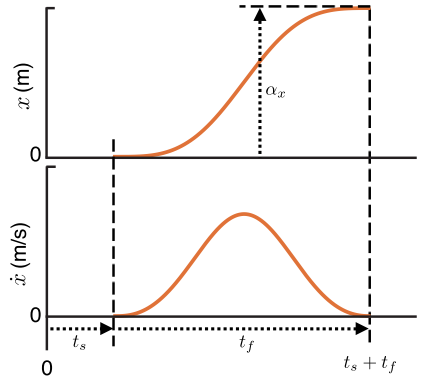

FIGURE 1. Definition of time parameters in the proposed trajectory generation model. In this example, the time at the data starting point is zero. Parameter t_s is the reaching start time, which is defined for the data starting point as a reference. If the reaching start time exists outside of the data due to processes such as data extraction, t_s can take a negative value. Parameter t_f is the reaching end time, which is defined for t_s as a reference. Therefore, the time required from the data starting point to the end of the reaching movement is $t_s + t_f$.

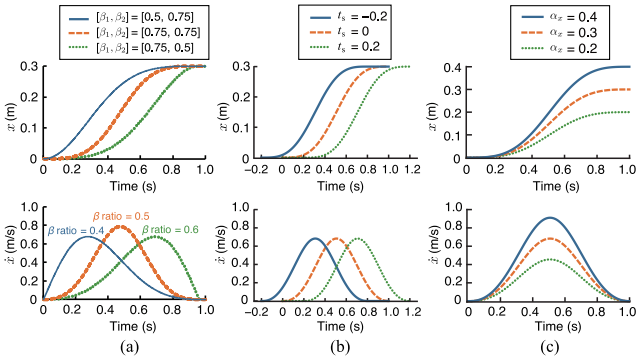

FIGURE 2. Time histories of x and $\dot{x}$ with changing parameters. (a) Parameters $[\beta_1, \beta_2]$ are set to [0.75, 0.5], [0.75, 0.75], and [0.5, 0.75]. (b) Parameter t_s is set to −0.2, 0, and 0.2. (c) Parameter α_x is set to 0.2, 0.3, and 0.4.

introducing the start time parameter t_s (Fig. 2(b)) and the distance-traveled parameter α_x (Fig. 2(c)).

Evaluating the velocity waveforms obtained from the three-dimensional position coordinates is necessary because actual reaching movements are performed in a three-dimensional space. Thus, the one-dimensional model, defined by (4), was applied to each axis of the three dimensions. The trajectory generation model for the three-dimensional hand position (x, y, z) was defined as follows:

$$\begin{bmatrix} \dot{x} \\ \dot{y} \\ \dot{z} \end{bmatrix} = \begin{bmatrix} \alpha_x \gamma_x \xi_x^{\beta_{1x}} (1-\xi_x)^{\beta_{2x}} \\ \alpha_y \gamma_y \xi_y^{\beta_{1y}} (1-\xi_y)^{\beta_{2y}} \\ \alpha_z \gamma_z \xi_z^{\beta_{1z}} (1-\xi_z)^{\beta_{2z}} \end{bmatrix}. \tag{8}$$

Fig. 3 shows the trajectory of the three-dimensional hand position (x, y, z) and the velocity waveform $(\dot{x}, \dot{y}, \dot{z})$ when β_{1l} and β_{2l} are changed (for $l \in \{x, y, z\}$). The other parameters are set to $\alpha_l = 0.3$ and $t_f = 1$. We confirmed that adjusting β_1 and β_2 in each axis changed the shape of the velocity waveform of each axis and generated arcuate or S-shaped trajectories.

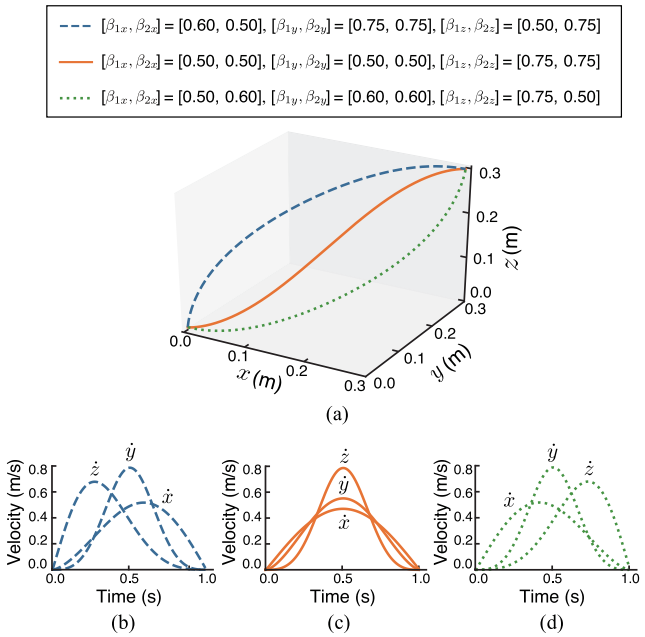

FIGURE 3. Trajectories of x, y, and z and the time histories of $\dot{x}$, $\dot{y}$, and $\dot{z}$. (a) The trajectories generated for each set of β_{1l} and β_{2l} (for $l \in \{x, y, z\}$). (b) The velocity waveforms of the dashed-line trajectory. (c) The velocity waveforms of the solid-line trajectory. (d) The velocity waveforms of the dotted-line trajectory. The other parameters are set to $\alpha_l = 0.3$, $t_s = 0$, and $t_f = 1$.

As described above, we constructed a reaching trajectory generation model capable of fitting to the measured data by introducing start time and travel distance parameters into the TBG.

C. PARAMETER ESTIMATION

This subsection describes the parameter estimation method of the proposed trajectory generation model. First, to achieve a robust estimation that can account for experimental data containing noise, the loss function $\rho(\cdot)$ based on Tukey's biweight estimation method [20] was defined as follows:

$$\rho(e) = \begin{cases} \dfrac{k^2}{6}\left\{1 - \left[1 - \left(\dfrac{e}{k}\right)^2\right]\right\} & |e| \le k \\ \dfrac{k^2}{6} & |e| > k. \end{cases} \tag{9}$$

Here, the residual e is the difference between the measured value and the value estimated by the model, and k is an arbitrary constant used to set the acceptable range for outliers.

Let us consider the estimation of the proposed model parameters, given N samples of the velocity signal $(\dot{x}_n, \dot{y}_n, \dot{z}_n; n = 1, \ldots, N)$ obtained from the time-series data of the three-dimensional hand position. First, by using only the x-axis data, the parameters α_x, t_s, t_f, β_{1x}, and β_{2x} can be estimated by minimizing

$$J = \sum_{n=1}^{N} \rho(\dot{x}_n - \hat{\dot{x}}_n) \tag{10}$$

for the predicted value $\hat{\dot{x}}_n$ with the proposed model. For the y-axis and z-axis data, the parameters can be estimated by solving the same optimization problem as for the x-axis data.

To minimize the evaluation function, the trust-region reflective (TRF) method was adopted [21], which is a method that can solve the nonlinear least-squares problems with bound constraints. This algorithm iteratively solves augmented trust-region subproblems, and the shape of the trust-region is determined by the distance from the bounds and the direction of the gradient. This helps to avoid direct steps into bounds and to efficiently explore the entire parameter space. The upper and lower bound constraints for the parameters can be set by applying the TRF method to avoid impractical values [22]. Using this method therefore allows for the more efficient and robust optimization of the nonlinear least-squares problem relative while satisfying $0 < \beta_i < 1$ $(i = 1, 2)$, which is the constraint of the parameters β_1 and β_2. The parameters of the proposed model can thus be estimated from the measured three-dimensional position data.

III. EXPERIMENTS

A. SIMULATION

To verify the estimation accuracy of the proposed model, a simulation experiment was conducted using artificially generated one-dimensional velocity waveform data. In the observed reaching data, the waveform was extracted at a rate of 5%–20% of the peak velocity in many instances. The waveform also contains noise attributable to external factors. Therefore, this simulation experiment was conducted to verify whether the proposed method would retain robust parameter estimation against these influences.

One-dimensional artificial data $\dot{x}$ were generated using (4), and they were regarded as the velocity waveforms observed during the reaching movement at a sampling frequency of 100 Hz. The parameters α, t_f, β_1, and β_2 were estimated for the generated $\dot{x}$ with the proposed method. The accuracy was verified by comparing the true parameters used at the generation of $\dot{x}$ with the estimated parameters. The absolute percentage error was used as an index of estimation accuracy and was defined as |true value − estimated value|/(true value) × 100. Here, the arbitrary constant k for the parameter estimation was set to $k = 4.685\sigma_e$ by using the standard deviation σ_e of the residual e [23]. The optimization constraint conditions are set to $-0.5 < t_s$, $0 < t_f$, and $0 < \beta_i < 1$ with the TRF method.

The robustness against the partial extraction of the waveform was then investigated. The W % of the peak velocity was set as the reference threshold; only velocity waveforms above this threshold were used to estimate the parameters. The average absolute percentage errors were calculated by changing the true value of the parameter 225 times ($\alpha = 0.2, 0.25, 0.3$, $t_s = 0$, $t_f = 1.0, 1.3, 1.6$, $\beta_i = 0.3, 0.4, \ldots, 0.7$). The data cutting rate with respect to peak velocity was set to $W = 0\%$, 5%, 10%, and 20%.

We then considered the robustness of the model against noise. Data points corresponding to L % of the total data

length in artificial data $\dot{x}$ were selected at random, and noise following the normal distribution with a mean of 0 and a standard deviation of s was added to each point of L % of the total data $\dot{x}$. Parameter estimation was then conducted with the velocity waveform data after adding the noise. The average absolute percentage error was calculated by changing the true value of the parameter nine times ($\alpha = 0.3$, $t_s = 0$, $t_f = 1.0$, $\beta_i = 0.4, 0.5, 0.6$). The noise addition rate L with respect to the data length and the standard deviation s of the noise were set to $L = 10\%, 30\%, 50\%, 70\%$, and 100%; and $s = 0.01, 0.02, \ldots, 0.05$; respectively.

B. THREE-DIMENSIONAL REACHING DATA ANALYSIS

Parameter estimation was conducted with three-dimensional reaching data. In general, the trajectory of the proficient reaching movement becomes almost linear [11]. In the proposed model, the trajectory generated by (8) becomes a straight line, if both $\beta_{1x} = \beta_{1y} = \beta_{1z}$ and $\beta_{2x} = \beta_{2y} = \beta_{2z}$ are satisfied. Thus, assuming a straight trajectory, if a human uses the TBG to generate a reaching trajectory in the brain, then the common β_1 and β_2 could possibly be planned in the three-dimensional space. The start and end times of the reaching motion are also common to each axis during reaching movement. Therefore, by setting the common reaching start time t_s, reaching end time t_f, β_1, and β_2 to each axis, the proposed model assuming a straight trajectory can be defined as follows:

$$\begin{bmatrix} \dot{x} \\ \dot{y} \\ \dot{z} \end{bmatrix} = \begin{bmatrix} \alpha_x \gamma_x \xi^{\beta_1} (1-\xi)^{\beta_2} \\ \alpha_y \gamma_y \xi^{\beta_1} (1-\xi)^{\beta_2} \\ \alpha_z \gamma_z \xi^{\beta_1} (1-\xi)^{\beta_2} \end{bmatrix}. \tag{11}$$

Parameter estimation was conducted with three-dimensional reaching data by using the proposed model and the proposed model assuming a straight trajectory. The results of the two models were then compared. Details of the derivation of the model assuming a straight trajectory and its parameter estimation method are provided in the Appendix.

We used the data reported by Corbett *et al.* [24] in the Database for Reaching Experiments and Models (DREAM).[1] In their experiment, six individuals each performed two reaching movements towards 18 target positions; our experiment only used the data collected during the training sessions to target the natural reaching movements. The data were digitally filtered by a second-order Butterworth zero-phase filter with a low-pass cutoff of 10 Hz. The arbitrary constant k and the optimization constraint condition for parameter estimation were set in the same manner as in the first experiment.

First, the fitting accuracy of the proposed model for three-dimensional data was evaluated. Here, the root mean square error (RMSE) between the measured velocity waveforms and the estimated velocity waveforms was calculated for each of the proposed models (i.e., the proposed model with independent fitting for each axis and the proposed model assuming a straight trajectory). When comparing RMSEs between models, the paired t-test was conducted with a significance level of 0.1%. The effect size d [25] was also calculated. The index d represents the magnitude of the difference between two average values by normalizing the difference between them. In general, a small effect is $0.2 \leq d < 0.5$, a moderate effect is $0.5 \leq d < 0.8$, and a large effect is $0.8 \leq d$. To test the hypothesis that β_1 and β_2 would be common to each axis when straight trajectories are assumed, the β ratios were calculated with β_1 and β_2 estimated using the model assuming a straight trajectory and with β_1 and β_2 for each axis estimated using the model in which the parameters are independent in the three dimensions. Two one-sided t-tests (TOSTs) [26], [27] were used to test the mean equivalency of the β ratios between models. The variable ϵ, defined as the allowable difference in the TOSTs, was set to 0.05: 5% of the possible range of the β ratio.

C. ONE-DIMENSIONAL REACHING DATA ANALYSIS

This experiment was conducted to compare the fitting accuracy of the proposed model with the conventional reaching trajectory generation model and to analyze the relationship between the model parameters and the physical features during the reaching movement.

One-dimensional reaching data collected by Vahdat *et al.* [28] and deposited in the DREAM were used as data to be fitted by the models. In their experiment, 13 individuals (aged 21–44 years) participated and performed 100 reaching movements towards a stationary target [28]. Our experiment used reaching data collected in the absence of an external force. These data were obtained during reaching movements in the y-axis direction on the horizontal plane; therefore, only data in the y-axis direction were used for this analysis. The data were digitally filtered in the same manner as in the second experiment. The constant k and the optimization constraint condition for parameter estimation were set in the same manner as in the first and second experiments.

The support-bounded lognormal model (SBL), the most accurate of 23 reaching trajectory models [29], was compared with the proposed model. The velocity waveform V_σ of the SBL was defined as follows:

$$V_\sigma = \begin{cases} \dfrac{P_1}{(t-P_2)(P_3-t)} e^{-P_4\left[\ln\left(\frac{(t-P_2)}{(P_3-t)}\right)-P_5\right]^2} & T_0 \leq t \leq T_1 \\ 0 & \text{otherwise,} \end{cases} \tag{12}$$

where T_0 and T_1 are defined as the movement start and end times. Here, P_i ($i = 1, 2, \ldots, 5$) is the parameter of the SBL. The relationship between the SBL parameters and the reaching movement features can be interpreted as follows [30]:

$$\text{Distance} = \frac{P_1}{P_3 - P_2}\sqrt{\frac{\pi}{P_4}}, \tag{13}$$

$$\text{Reaching start time} = P_2, \tag{14}$$

$$\text{Reaching end time} = P_3. \tag{15}$$

[1]The datasets are available at CRCNS: https://crcns.org/data-sets/movements/dream

The SBL is an extension of lognormal distribution; therefore, the parameters μ and σ of lognormal distribution can be represented with the parameters P_4 and P_5 of the SBL as $\mu = P_5$ and $\sigma = \sqrt{1/(2P_4)}$, respectively. For the parameter estimation of the SBL, we used the Levenberg-Marquardt method [31]: similar to the method described by Plamondon *et al.* [29], it is used to solve the problem of nonlinear least-squares.

Parameter estimation was first conducted with one-dimensional data. The RMSEs between the measured velocity waveforms and those estimated with the proposed model and the SBL were calculated and compared. A paired t-test with a significance level of 1% was used to compare the RMSEs between models. The effect size d [25] was also calculated. Moreover, the relationships between the parameters of the proposed model and the physical features during reaching movement were analyzed using linear regression analysis between the estimated parameters α, $t_s + t_f$, β ratio, and γ of the proposed model, and the reaching traveled distance, data length, peak velocity time, and peak velocity obtained from the reaching data. For the SBL, a linear regression analysis was likewise conducted to test the relationships of (13) and (15), and between P_5 corresponding to parameter μ of the lognormal distribution and peak velocity time. The peak velocity time was normalized using the reaching data length. Finally, to evaluate the shape of the velocity waveform, the β ratio of the proposed model was analyzed.

IV. RESULTS

A. PARAMETER ESTIMATION ACCURACY

Fig. 4 shows examples of the artificial velocity waveforms and the estimated velocity waveforms obtained with the proposed model when the data cutting rate W was set to 0%, 5%, 10%, and 20%. Fig. 5 shows the average absolute percentage errors of parameters α, t_f, β_1, and β_2 for each data cutting rate W. Fig. 6 shows examples of the artificial velocity waveforms and the estimated waveforms obtained using the proposed model when the standard deviation s was set to $s = 0.01$ (Fig. 6(a)) and $s = 0.05$ (Fig. 6(b)) and the noise addition rate L was changed to 10%, 50%, and 100% for each value of s. Fig. 7 shows the mean absolute percentage errors of the parameters α, t_f, β_1, and β_2 for the standard deviation s and for the noise addition rate L.

B. ANALYSIS OF THREE-DIMENSIONAL REACHING MOVEMENT DATA

Fig. 8 shows examples of the measured and estimated velocity waveforms in each model fitted independently to each axis and assuming a straight trajectory. Fig. 9(a) shows the mean and standard deviation of the RMSEs for each model fitted independently to each axis and assuming a straight trajectory. The p value from the paired t-test and the effect size d are also presented, and a significant difference is observed ($p < 0.001$). Fig. 9(b) shows the mean and standard deviation of the β ratio calculated from the estimated parameters β_1 and

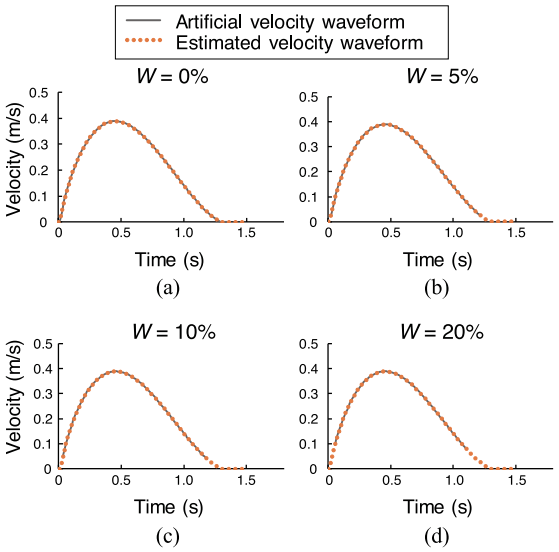

FIGURE 4. Examples of artificial and estimated velocity waveforms with the data cutting rate W set to (a) 0%, (b) 5%, (c) 10%, and (d) 20%.

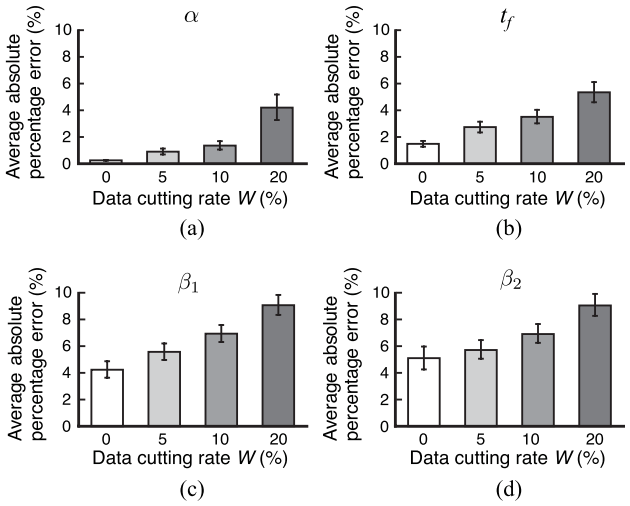

FIGURE 5. Average absolute percentage errors for each data cutting rate W in the estimation of (a) α, (b) t_f, (c) β_1, and (d) β_2. Error bars represent 95% confidence intervals for all trials.

β_2 with each model. The TOSTs results are also presented in the figure. The β ratios obtained when fitting the model independently for each axis and when assuming a straight trajectory were significantly equivalent ($p < 0.001$).

C. ANALYSIS OF ONE-DIMENSIONAL REACHING MOVEMENT DATA

Fig. 10 shows examples of the measured velocity waveforms and those estimated with the proposed model and the SBL. The estimated parameters of each model corresponding to the reaching start and end times are also shown. The RMSEs calculated in the examples was 0.0164 m/s for the proposed model and 0.0031 m/s for SBL. Fig. 11 shows the RMSE results for the proposed model and the SBL. The paired t-test results and the effect size d are also shown. We found

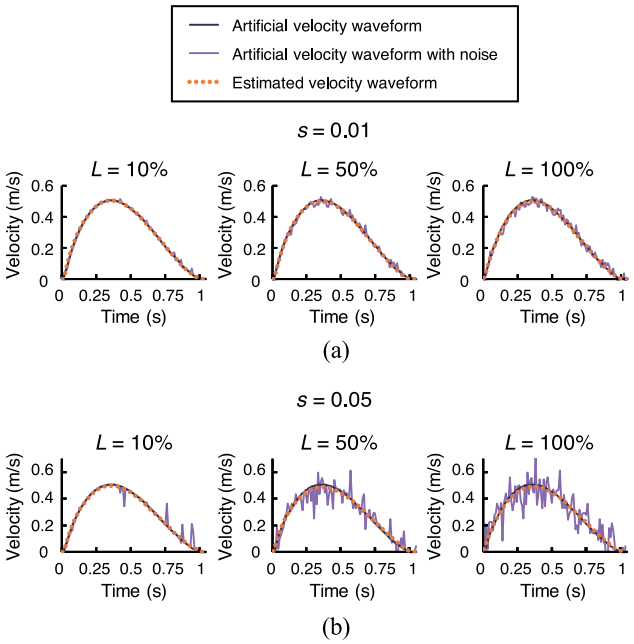

FIGURE 6. Examples of artificial velocity waveforms, artificial velocity waveforms with noise, and estimated velocity waveforms for each noise addition rate L. The standard deviation s for noise generation was set to (a) $s = 0.01$ and (b) $s = 0.05$.

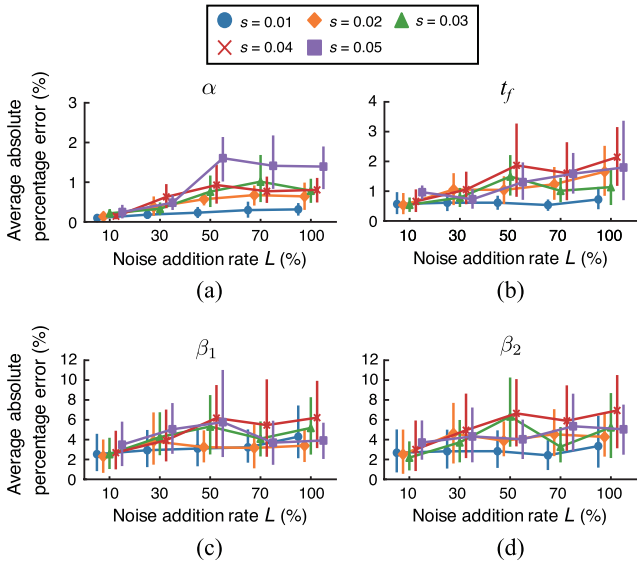

FIGURE 7. Average absolute percentage errors for each noise addition rate L in the estimation of (a) α, (b) t_f, (c) β_1, and (d) β_2. For each, the standard deviation s for noise generation was set to $s = 0.01, 0.02, \ldots, 0.05$. Error bars represent 95% confidence intervals for all trials.

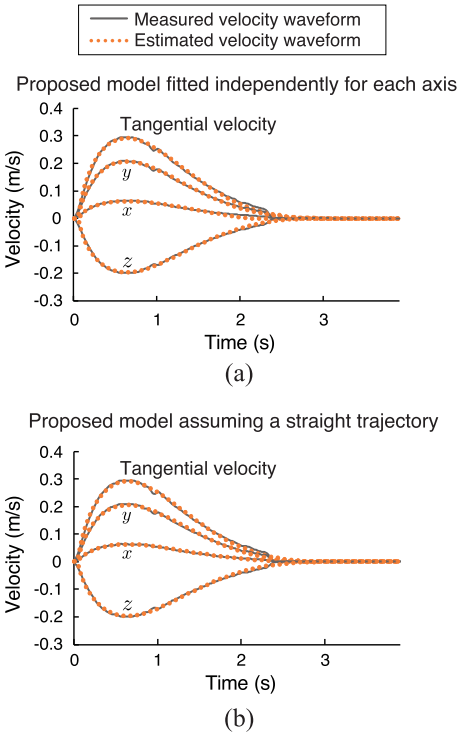

FIGURE 8. Examples of measured and estimated velocity waveforms. (a) The proposed models fitted independently for each axis. (b) The proposed model assuming a straight trajectory.

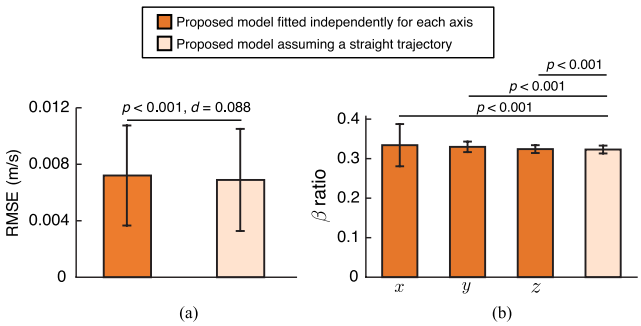

FIGURE 9. Comparison of the results between the proposed model fitted independently and the proposed model assuming a straight trajectory. (a) Root mean square error (RMSE) for tangential velocities of each model. Error bars represent the standard deviations for all trials. The p value from the paired t-test and the effect size d are also shown. (b) β ratio of each model. Error bars represent the standard deviations for all trials. The p values from the two one-sided t-tests (TOSTs) are also shown.

a significant difference between the RMSEs of the models ($p < 0.01$).

The box plots in Fig. 12 show the parameters estimated with the proposed model and the SBL. Fig. 13 shows the relationship between the parameters estimated with the proposed model and the physical features obtained from the actual reaching data. The data in the scatter plots indicate the relationships between the distance parameter α and the reaching traveled distance; between the reaching convergence time $t_s + t_f$, when the time was matched to the actual measurement data, and the reaching data length; between the β ratio and the normalized peak velocity time; and between the γ parameter and the peak velocity. Fig. 14 presents scatterplots that show the relationships between the SBL distance (13) and the reaching traveled distance, between the convergence time parameter P_3 and the reaching data length, and between parameter P_5 corresponding to μ in the lognormal distribution and the normalized peak velocity time. In each figure,

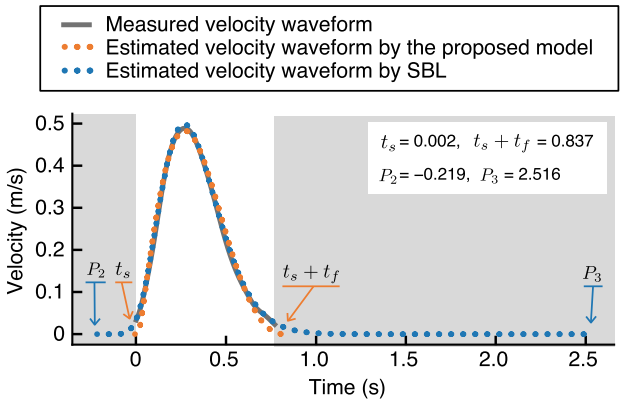

FIGURE 10. Examples of measured and estimated velocity waveforms. The solid dark gray line represents the measured velocity waveform. Orange and blue dotted lines represent velocity waveforms estimated with the proposed model and the SBL, respectively. Light gray areas represent the outer part of the measured data. The estimated parameters of each model corresponding to the reaching start and end times are also shown.

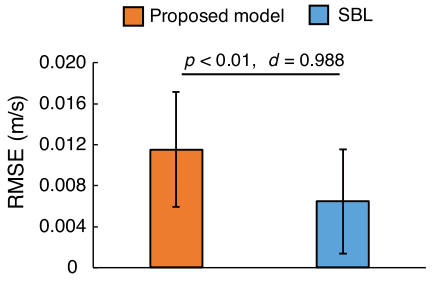

FIGURE 11. Root mean square errors (RMSEs) of the proposed model and support-bounded lognormal (SBL) model. Error bars represent the standard deviations for all trials. The *p* value from the paired *t*-test and the effect size *d* are also shown.

the determination coefficient R^2 and p value obtained from linear regression analysis are also shown.

Fig. 15 shows the box plots of the β ratio calculated from data from all participants (Fig. 15(a)) and the β ratio calculated for each participant (Fig. 15(b)). The 95% confidence interval of the β ratio for all participants was 0.452–0.457. Fig. 16 shows the velocity waveforms of the first 10 reaching movements of Participant 7 and Participant 8.

V. DISCUSSION

The present investigation proposes a spatiotemporal parameterization method that allows for the evaluation of reaching movements with a trajectory generation model based on the TBG. The simulation experiment confirmed that the proposed model fitted well to artificial data extracted at the thresholds based on the peak velocity and that the outside of the extraction range was well-extrapolated (Fig. 4). Moreover, as shown in Fig. 5, the average absolute percentage errors when using the total data length ($W = 0\%$) were, at most, approximately 5% for α, t_f, β_1, and β_2 This finding indicates that the proposed method can accurately estimate the parameters. The estimation accuracy tended to gradually decrease in accordance with the increase in the data cutting rate W to 5%,

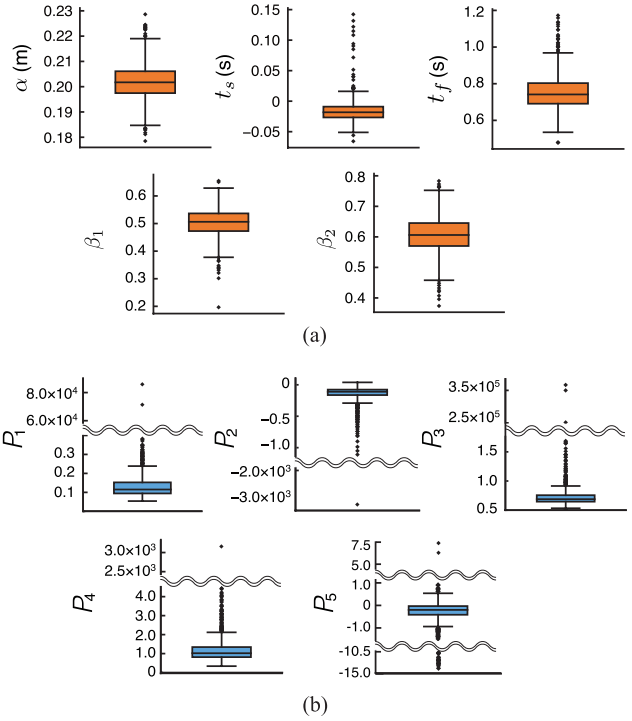

FIGURE 12. Box plots of the estimated parameters. (a) The proposed model. (b) The support-bounded lognormal (SBL) model. The solid horizontal line in each box plot indicates the median value of each parameter.

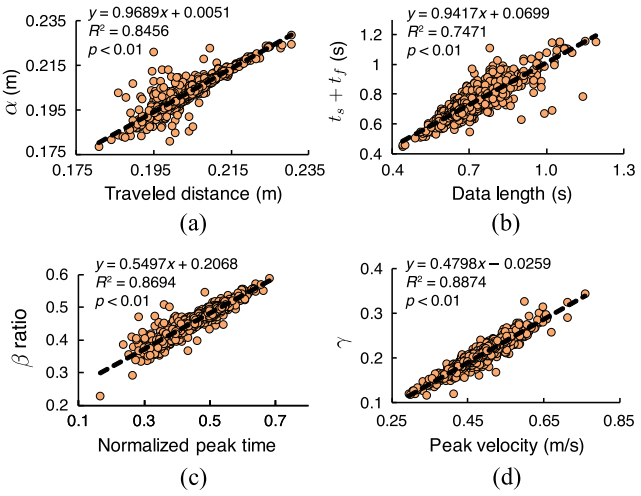

FIGURE 13. Scatter plots of the estimated parameters and physical features extracted from the reaching data based on the proposed model. (a) The target distance α and the traveled distance. (b) The end time plus start time $t_s + t_f$ and the data length. (c) The β ratio and the normalized peak time. (d) The parameter γ and the peak velocity. Dashed lines represent regression lines. The regression equations and coefficients of determination are also shown.

10%, and 20%. Therefore, the average absolute percentage errors were less than 10%, even in the case of $W = 20\%$. This finding could be attributed to our adoption of TRF—a robust method based on a confidence region method—as our nonlinear least-squares method. These results demonstrate that the proposed method can be used to estimate the parameters

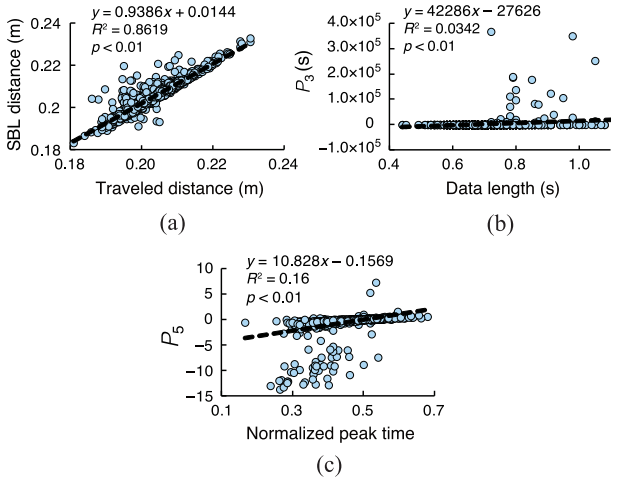

FIGURE 14. Scatter plots of the estimated parameters and physical features extracted from the reaching data with the support-bounded lognormal (SBL) model. (a) The distance calculated with the SBL parameters and the traveled distance. (b) The parameter P_3 and the data length. (c) The parameter P_5 and the normalized peak time. Dashed lines represent regression lines. The regression equations and coefficients of determination are also shown.

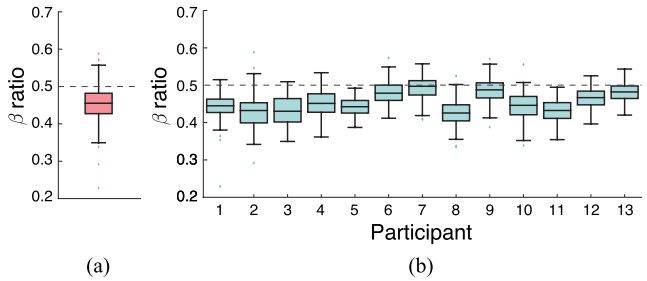

FIGURE 15. Box plots of β ratios with data from (a) all participants and (b) each participant. Solid horizontal lines in each box plot denote the median value of the β ratio. Dashed horizontal lines indicate the positions for which the β ratio is 0.5.

with high accuracy, even for velocity waveforms extracted at thresholds based on peak velocity.

As shown in Fig. 6, the percentage error tended to increase in accordance with the increase in the standard deviation s of noise and the noise addition rate L; however, the percentage error of each parameter was less than 10%. This finding indicates the robustness of the parameter estimation of the model, even with noisy data. Moreover, even when large noise was added to the rear of the velocity waveform, as shown in Fig. 6(b), the estimated velocity waveform could capture the characteristics of the waveform before adding the noise. This finding may be attributed to our adoption of a loss function based on Tukey's biweight estimation method, which sets the weight according to the degree of data deviation and thus enables robust estimation against noise.

The aforementioned findings indicate that the proposed method achieved a high parameter estimation accuracy for the one-dimensional artificial velocity waveform, even following waveform extraction or noise addition.

The fitting experiment using three-dimensional reaching data revealed a significant difference between the RMSEs

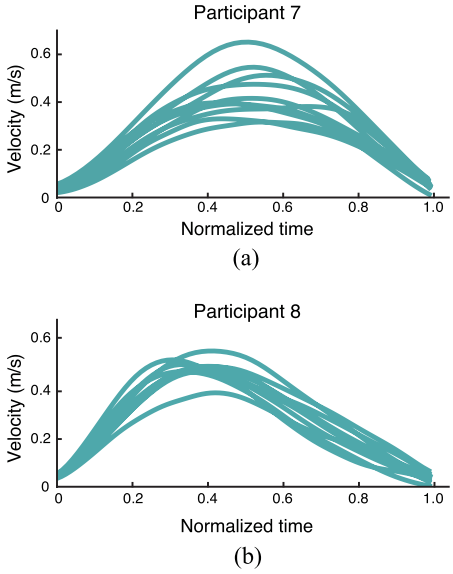

FIGURE 16. Examples of velocities of the first 10 reaching movements during the experiment of (a) Participant 7 and (b) Participant 8.

of the proposed model fitted independently to each axis and the proposed model assuming a straight trajectory (Fig. 9(a)). However, the effect size d was 0.088, indicating a small difference. This finding could be attributed to much of that data having been collected from straight reaching movements. Therefore, the proposed model can accurately fit the velocity waveform data, even in the model assuming a straight trajectory, with respect to three-dimensional data and the use of common parameters for each axis.

In Fig. 9(b), the estimated β ratios were smaller than the value of 0.5, which represents asymmetry of the velocity profile. Here, β_1 and β_2 are parameters controlling the shape of the velocity waveform, and the β ratio represents the position of the peak velocity time (see Section II. B). Therefore, the peak velocity time of the data is closer to the reaching start time than to the midpoint in velocity waveforms. This tendency can be also seen from the velocity waveforms in Fig. 8. In addition, the results of the TOSTs indicate that the β ratios calculated from the proposed model fitted independently to each axis and the proposed model assuming a straight trajectory were significantly equivalent.

These results suggest that the shape of the velocity waveform becomes nearly equal on each axis in reaching movements in three-dimensional space. We thus confirmed that setting parameters common to three-dimensional space in the proposed trajectory generation model assuming a straight trajectory is reasonable.

The fitting experiment using one-dimensional reaching data revealed a significant difference between the RMSEs of the proposed model and the SBL, with a large effect size ($d = 0.998$) (Fig. 11). This finding suggests that the SBL is more accurate than the proposed model in terms of the residuals. However, as shown in Fig. 12(b), the estimation result of the SBL parameters featured a very large variation. In particular, P_3, which represents the end time of

the reaching movement, contained many extreme outliers. Thus, the RMSE of the SBL is smaller than that of the proposed model because the SBL overfitted the measured data. By contrast, in the proposed method, the variation of the estimated parameters was small, indicating a more robust parameter estimation (Fig. 12(a)). The SBL model is based on lognormal distribution, which itself is supported by a semi-infinite interval. In the SBL, the lognormal distribution is bounded by defining the reaching start and end times, P_2 and P_3, assuming that the data contains points with zero velocity corresponding to the reaching start and end times. Therefore, these parameters could not be successfully estimated and had taken extremely large or small values for the extracted waveforms based on the ratio of the peak velocity. The other parameters (i.e., P_1, P_4, and P_5) also exhibited large variation due to the influence of instability in the estimation of P_2 and P_3. Consequently, although the RMSE of SBL is small, its parameters may take extreme values. By contrast, since the proposed model based on the TBG is supported by bounded intervals, the parameters may be estimated with greater stability even in the case of extracted data. In addition, the combination of TRF and Tukey's biweight loss function in the parameter optimization of the proposed method also contributed to the robustness of the estimated parameters (see Supplementary Material).

Based on the regression analysis between the estimated parameters and physical features, the parameters of the proposed model showed a higher coefficient of determination for the reaching data length and normalized peak time than that of the SBL, although a higher coefficient of determination was detected for the traveled distance parameter of the SBL than that of the proposed model (Figs. 13 and 14). The many extreme outliers caused by overfitting to the measured data accounts for the low coefficient of determination between P_3 and the reaching data length and between P_5 and the normalized peak time in the results of the SBL. However, in the proposed model, the variation in the estimated parameters was small, and linear regression analysis revealed that all coefficients of determination were higher than 0.7. This finding indicates that the physical features of reaching movements can be evaluated using the estimated parameters of the proposed model. We can therefore conclude that the proposed model is superior in terms of the parameterization of reaching movement features.

As shown in Fig. 15(a), the β ratio obtained from all participants was distributed around a value smaller than 0.5, which means the velocity waveform is asymmetrical. In addition, the 95% confidence interval was 0.452–0.457, suggesting that the peak velocity time of the velocity waveform occurs, on average, before the midpoint of the movement. This trend was also seen in the data used in the second experiment (as shown in Fig. 9(b)). Our results also support previous findings demonstrating that the velocity waveforms of reaching movements sometimes lose symmetry [10].

In Fig. 15(b), the distribution of the β ratio differed between individuals. Participant 7 showed a median β ratio of nearly 0.5, and Participant 8 exhibited β ratios that were distributed with a smaller median value. This tendency was also observed in the velocity waveforms of the actual measurement data. The peak of the velocity waveform in Participant 7 was close to the center (Fig. 16(a)), whereas that of Participant 8 was closer to the left of the center (Fig. 16(b)). While some previous works have evaluated the features of individuals' lower limb movement [32], [33], upper limb reaching movements have rarely been considered. Furthermore, analyses on reaching movements have focused primarily on changes caused by the environment [8], [10]. Marteniuk *et al.* reported that knowledge based on past experiences might influence reaching movements [8]. Therefore, past experience, physical characteristics, and age manifest as individual differences in reaching movement. However, such individual differences have rarely been analyzed. Our experimental results revealed that the tendency of the bell-shaped velocity waveform of the reaching movement differs for each individual. In addition, individual differences can be quantitatively evaluated as the difference in the β ratio, which represents the shape of the velocity waveform. Hence, if a human uses the TBG for trajectory generation in the brain, the reaching movement can be performed by using a specific β ratio optimized for an individual. By using the proposed method, the characteristics of individual reaching movements can be parameterized and evaluated.

The method proposed in this paper aims to parameterize a simple reaching movement. However, some of the more complex upper-limb movements exhibit bell-shaped velocity waveforms, such as those seen during reaching movements. For example, Oubre *et al.* showed that the segmented velocity profile during random (patternless) voluntary upper-limb movements featured an approximately bell-shaped morphology [34]. In addition, Miranda *et al.* suggested that complex upper-limb movements can be modeled as a combination of simple reaching movements with a bell-shaped velocity profiles [35]. Therefore, it would be possible to achieve the quantitative analysis of various types of upper-limb movements based on the proposed method by interpreting complex movements as approximate reaching movements or a sequence of reaching movements.

VI. CONCLUSION

This study proposes a spatiotemporal parameterization method to analyze the human reaching movements. With the proposed method, the features of the velocity waveform during the reaching movement can be quantitatively acquired by fitting a reaching trajectory generation model based on the TBG [17] to the measured reaching data and subsequently estimating the parameters. The proposed method could potentially benefit the clinical evaluation of a patient's motor function during rehabilitation and the development of user interface designs.

By verifying the accuracy of parameter estimation using artificially generated velocity waveform data, we confirmed that the average absolute error rate was approximately 5% at

most. Furthermore, parameter estimation can be conducted with an average absolute error rate of less than 10%, even when velocity waveform extraction and noise addition are conducted with the generated artificial data. The parameter estimation experiment performed with real-world three-dimensional reaching data revealed that the measured velocity waveforms could be fitted accurately, even when assuming a straight trajectory in the model and using parameters common to each axis. Regarding real-world one-dimensional reaching data, we found that the estimated parameters of the proposed model featured less variation than that of the conventional model and could be estimated more robustly. The present study observed strong correlations between the estimated proposed model parameters and the physical features extracted from the measured data. We thus concluded that the reaching movement can be quantitatively evaluated using the estimated parameters.

In addition, based on the distribution of the β ratio calculated from the estimated parameters of all participants, the peak velocity time of the velocity waveform was, on average, situated left of center. We also identified individual differences in the distribution of the β ratio among participants. These findings indicated that the proposed method could be used to parameterize the characteristics of individual reaching movements.

The data used in this study were acquired from healthy participants who performed straight reaching movements. To verify the general applicability of the proposed parameterization method, further analysis of different kinds of data is warranted. Because the parameters β_1 and β_2 of the proposed model change on each axis in nonlinear reaching movements in three-dimensional space, the nonlinearity and the shape of the velocity waveform could potentially be evaluated concurrently by elucidating β_1 and β_2 on each axis. We therefore plan to analyze nonlinear reaching movements using the proposed parameterization method in future research. In addition, we will analyze changes in the estimated parameters for the separated groups according to participant characteristics or measurement environments to determine the type of factor that affects the changes in the reaching movement. As described at the end of Section V, the proposed method can be applied to both simple reaching movements and more complex movements. We plan to verify the efficacy of the proposed method by analyzing more complex movements that can be interpreted as approximate reaching movements in future research.

APPENDIX

Let us consider the necessary and sufficient condition that a trajectory generated by (8) becomes straight. Based on the reaching movement in the xy-plane, the necessary and sufficient condition in which the model becomes a straight trajectory at the reaching hand position (x, y) in plane is that dy/dx is a constant and is expressed by the following equation:

$$\frac{dy}{dx} = \frac{\alpha_y \gamma_y \xi_y{}^{\beta_{1y}} (1-\xi_y)^{\beta_{2y}}}{\alpha_x \gamma_x \xi_x{}^{\beta_{1x}} (1-\xi_x)^{\beta_{2x}}}. \tag{16}$$

Here, as indicated in (16), if t_s and t_f in x and y are equal, and $\beta_{1x} = \beta_{1y}$ and $\beta_{2x} = \beta_{2y}$ are satisfied, then dy/dx becomes equal to a constant α_y/α_x. For each set of (x, y, z), the necessary and sufficient condition that the trajectory becomes straight in (8) is that the reaching start time t_s and the end time t_f are common for each axis, and $\beta_{1x} = \beta_{1y} = \beta_{1z}$ and $\beta_{2x} = \beta_{2y} = \beta_{2z}$ are satisfied. Therefore, the trajectory generation model for the three-dimensional hand position when assuming a linear trajectory can be derived (11) by setting a common reaching start time t_s, the end time t_f, β_1, and β_2 to each axis.

Considering the case of (11), which assumes a three-dimensional linear trajectory, each axis direction features common parameters. Therefore, optimizing three-dimensional velocity waveforms is necessary. Now consider the estimation of model parameters, given N samples of the three-dimensional hand position data $(\dot{x}_n, \dot{y}_n, \dot{z}_n; n = 1, \ldots, N)$. Let the prediction value of the proposed model be $(\hat{\dot{x}}_n, \hat{\dot{y}}_n, \hat{\dot{z}}_n)$ and a loss function (9) based on Tukey's biweight estimation method [20] be used as the eveluation function as follows:

$$J = \sum_{n=1}^{N} \rho(\dot{x}_n - \hat{\dot{x}}_n) + \sum_{n=1}^{N} \rho(\dot{y}_n - \hat{\dot{y}}_n) + \sum_{n=1}^{N} \rho(\dot{z}_n - \hat{\dot{z}}_n). \tag{17}$$

By minimizing J, the parameters α_l (for $l \in \{x, y, z\}$), t_s, t_f, β_1, and β_2 can be estimated for three-dimensional hand position data. Capable of solving the problem of constrained nonlinear least-squares, the trust-region reflective (TRF) method [21] was used to minimize the evaluation function.

REFERENCES

[1] C. Bassano, F. Solari, and M. Chessa, "Studying natural human-computer interaction in immersive virtual reality: A comparison between actions in the peripersonal and in the near-action space," in *Proc. 13th Int. Joint Conf. Comput. Vis. Imag. Comput. Graph. Theory Appl.*, vol. 2, 2018, pp. 108–115.

[2] D. E. Holmes, D. K. Charles, P. J. Morrow, S. McClean, and S. M. McDonough, "Using Fitt's law to model arm motion tracked in 3D by a leap motion controller for virtual reality upper arm stroke rehabilitation," in *Proc. IEEE 29th Int. Symp. Comput.-Based Med. Syst. (CBMS)*, Jun. 2016, pp. 335–336.

[3] L. Rönnqvist and B. Rösblad, "Kinematic analysis of unimanual reaching and grasping movements in children with hemiplegic cerebral palsy," *Clin. Biomech.*, vol. 22, no. 2, pp. 165–175, Feb. 2007.

[4] E. Prytz, M. Montano, and M. W. Scerbo, "Using fitts' law for a 3D pointing task on a 2D display: Effects of depth and vantage point," in *Proc. Hum. Factors Ergonom. Soc. Annu. Meet.*, Los Angeles, CA, USA: SAGE Publications, vol. 56, no. 1, 2012, pp. 1391–1395.

[5] E. Jaspers, K. Desloovere, H. Bruyninckx, G. Molenaers, K. Klingels, and H. Feys, "Review of quantitative measurements of upper limb movements in hemiplegic cerebral palsy," *Gait Posture*, vol. 30, no. 4, pp. 395–404, Nov. 2009.

[6] A. de los Reyes-Guzmán, I. Dimbwadyo-Terrer, F. Trincado-Alonso, F. Monasterio-Huelin, D. Torricelli, and A. Gil-Agudo, "Quantitative assessment based on kinematic measures of functional impairments during upper extremity movements: A review," *Clin. Biomech.*, vol. 29, no. 7, pp. 719–727, Aug. 2014.

[7] E. A. Aboelnasr, F. A. Hegazy, and H. A. Altalway, "Kinematic characteristics of reaching in children with hemiplegic cerebral palsy: A comparative study," *Brain Injury*, vol. 31, no. 1, pp. 83–89, Jan. 2017.
[8] R. C. Marteniuk and C. L. Mackenzie, "Constraints on human arm movement trajectories," *Can. J. Psychol.*, vol. 41, no. 3, pp. 365–378, 1987.
[9] D. J. Ostry, J. D. Cooke, and K. G. Munhall, "Velocity curves of human arm and speech movements," *Exp. Brain Res.*, vol. 68, no. 1, pp. 37–46, Sep. 1987.
[10] H. Nagasaki, "Asymmetric velocity and acceleration profiles of human arm movements," *Exp. Brain Res.*, vol. 74, no. 2, pp. 319–326, 1989.
[11] P. Morasso, "Spatial control of arm movements," *Exp. Brain Res.*, vol. 42, no. 2, pp. 223–227, Apr. 1981.
[12] T. Flash and N. Hogan, "The coordination of arm movements: An experimentally confirmed mathematical model," *J. Neurosci.*, vol. 5, no. 7, pp. 1688–1703, Jul. 1985.
[13] Y. Uno, M. Kawato, and R. Suzuki, "Formation and control of optimal trajectory in human multijoint arm movement," *Biol. Cybern.*, vol. 61, no. 2, pp. 89–101, Jun. 1989.
[14] C. M. Harris and D. M. Wolpert, "Signal-dependent noise determines motor planning," *Nature*, vol. 394, no. 6695, pp. 780–784, Aug. 1998.
[15] D. Bullock and S. Grossberg, "VITE and FLETE: Neural modules for trajectory formation and postural control," *Adv. Psychol.*, vol. 62, pp. 253–297, Jan. 1989.
[16] P. Morasso, V. Sanguineti, and T. Tsuji, "A dynamical model for the generation of curved trajectories," in *Proc. Int. Conf. Artif. Neural Netw.* London, U.K.: Springer, Sep. 1993, pp. 115–118.
[17] T. Tsuji, Y. Tanaka, and M. Kaneko, "Bio-mimetic trajectory generation based on human arm movements with a nonholonomic constraint," *IEEE Trans. Syst., Man, Cybern. A, Syst., Humans*, vol. 32, no. 6, pp. 773–779, Nov. 2002.
[18] Y. Tanaka, T. Tsuji, V. Sanguineti, and P. G. Morasso, "Bio-mimetic trajectory generation using a neural time-base generator," *J. Robotic Syst.*, vol. 22, no. 11, pp. 625–637, 2005.
[19] T. Tsuji, Y. Tanaka, P. G. Morasso, V. Sanguineti, and M. Kaneko, "Bio-mimetic trajectory generation of robots via artificial potential field with time base generator," *IEEE Trans. Syst., Man, Cybern. C, Appl. Rev.*, vol. 32, no. 4, pp. 426–439, Nov. 2002.
[20] A. E. Beaton and J. W. Tukey, "The fitting of power series, meaning polynomials, illustrated on band-spectroscopic data," *Technometrics*, vol. 16, no. 2, pp. 147–185, May 1974.
[21] M. A. Branch, T. F. Coleman, and Y. Li, "A subspace, interior, and conjugate gradient method for large-scale bound-constrained minimization problems," *SIAM J. Sci. Comput.*, vol. 21, no. 1, pp. 1–23, Jan. 1999.
[22] T. M. Le, B. Fatahi, H. Khabbaz, and W. Sun, "Numerical optimization applying trust-region reflective least squares algorithm with constraints to optimize the non-linear creep parameters of soft soil," *Appl. Math. Model.*, vol. 41, pp. 236–256, Jan. 2017.
[23] J. Fox and S. Weisberg, "Robust regression in R," in *An R Comparison to Applied Regression*, 2nd ed. Thousand Oaks, CA, USA: Sage, 2011.
[24] E. A. Corbett, K. P. Kording, and E. J. Perreault, "Real-time fusion of gaze and EMG for a reaching neuroprosthesis," in *Proc. Annu. Int. Conf. IEEE Eng. Med. Biol. Soc.*, Aug. 2012, pp. 739–742.
[25] M. Borenstein, L. V. Hedges, J. P. Higgins, and H. R. Rothstein, *Introduction to Meta-Analysis*. Hoboken, NJ, USA: Wiley, 2011.
[26] D. L. Schuirmann, "On hypothesis-testing to determine if the mean of a normal-distribution is contained in a known interval," *Biometrics*, vol. 37, no. 3, p. 617, 1981.
[27] W. J. Westlake, "Bioequivalence testing—A need to rethink," *Biometrics*, vol. 37, no. 3, pp. 589–594, 1981.
[28] S. Vahdat, M. Darainy, T. E. Milner, and D. J. Ostry, "Functionally specific changes in resting-state sensorimotor networks after motor learning," *J. Neurosci.*, vol. 31, no. 47, pp. 16907–16915, Nov. 2011.
[29] R. Plamondon, A. M. Alimi, P. Yergeau, and F. Leclerc, "Modelling velocity profiles of rapid movements: A comparative study," *Biol. Cybern.*, vol. 69, no. 2, pp. 119–128, Jun. 1993.
[30] R. Plamondon, "Looking at handwriting generation from a velocity control perspective," *Acta Psychologica*, vol. 82, nos. 1–3, pp. 89–101, Mar. 1993.
[31] J. J. Moré, "The levenberg-marquardt algorithm: Implementation and theory," in *Numerical Analysis*. Berlin, Germany: Springer, 1978, pp. 105–116.
[32] J. E. Cutting and L. T. Kozlowski, "Recognizing friends by their walk: Gait perception without familiarity cues," *Bull. Psychonomic Soc.*, vol. 9, no. 5, pp. 353–356, May 1977.
[33] J. Lu, G. Wang, and P. Moulin, "Human identity and gender recognition from gait sequences with arbitrary walking directions," *IEEE Trans. Inf. Forensics Security*, vol. 9, no. 1, pp. 51–61, Jan. 2014.
[34] B. Oubre, J.-F. Daneault, H.-T. Jung, K. Whritenour, J. G. V. Miranda, J. Park, T. Ryu, Y. Kim, and S. I. Lee, "Estimating upper-limb impairment level in stroke survivors using wearable inertial sensors and a minimally-burdensome motor task," *IEEE Trans. Neural Syst. Rehabil. Eng.*, vol. 28, no. 3, pp. 601–611, Mar. 2020.
[35] J. G. V. Miranda, J.-F. Daneault, G. Vergara-Diaz, Â. F. S. D. O. Torres, A. P. Quixadá, M. D. L. Fonseca, J. P. B. C. Vieira, V. S. dos Santos, T. C. da Figueiredo, E. B. Pinto, N. Peña, and P. Bonato, "Complex upper-limb movements are generated by combining motor primitives that scale with the movement size," *Sci. Rep.*, vol. 8, no. 1, p. 12918, Aug. 2018.

MASANOBU KITTAKA received the B.E. and M.Eng. degrees from Hiroshima University, Hiroshima, Japan, in 2017 and 2019, respectively.

AKIRA FURUI (Member, IEEE) received the B.E., M.E., and D.Eng. degrees from Hiroshima University, Hiroshima, Japan, in 2016, 2018, and 2019, respectively.

He was a Research Fellow with the Japan Society for the Promotion of Science, from 2018 to 2019. He is currently an Assistant Professor with the Graduate School of Advanced Science and Engineering, Hiroshima University. His current research interests include biological signal analysis, human–machine interface, and stochastic modeling.

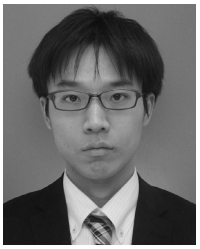

HIROTO SAKAI received the B.Eng. degree from Fukui University, Fukui, Japan, in 2019. He is currently pursuing the master's degree with the Graduate School of Engineering, Hiroshima University.

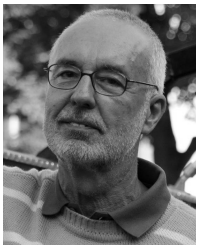

PIETRO MORASSO received the M.E. degree from the University of Genoa, in 1968.

He was a Research Fellow with MIT and a Full Professor in bioengineering with the University of Genoa. He is currently a Senior Researcher with the Istituto Italiano di Tecnologia. His current research interests include the neural control of movement, motor learning, robot therapy, and robot cognition.

TOSHIO TSUJI (Member, IEEE) received the B.E. degree in industrial engineering and the M.E. and D.Eng. degrees in systems engineering from Hiroshima University, Hiroshima, Japan, in 1982, 1985, and 1989, respectively.

He is currently a Full Professor with the Graduate School of Advanced Science and Engineering, Hiroshima University. His research interests range from engineering to human science, with focuses on cybernetics, medical electronics, computational neural sciences, and particularly biological Kansei modeling.

Dr. Tsuji has received 42 academic awards, including the IEEE 2003 King-Sun Fu Memorial Best Transactions Paper Award.